Clays and Clay Minerals, Vol. 48, No. 2, 272–281, 2000.

REDUCTION AND SORPTION OF CHROMIUM BY Fe(II)-BEARING PHYLLOSILICATES: CHEMICAL TREATMENTS AND X-RAY ABSORPTION SPECTROSCOPY (XAS) STUDIES

MARIA FRANCA BRIGATTI,[1] CRISTINA LUGLI,[1] GIANNANTONIO CIBIN,[2] AUGUSTO MARCELLI,[2] GABRIELE GIULI,[3] ELEONORA PARIS,[3] ANNIBALE MOTTANA,[4] AND ZIYU WU[5]

[1] Dipartimento di Scienze della Terra, Università di Modena e Reggio Emilia, via S. Eufemia 19, 41100 Modena, Italy
[2] I.N.F.N., Laboratori Nazionali di Frascati, P.O. Box 13, I-00044 Frascati, Italy
[3] Dipartimento di Scienze della Terra, Università di Camerino, Via Gentile III da Varano, I-62032 Camerino, MC, Italy
[4] Dipartimento di Scienze della Terra, Università di Roma 3, Largo S. Leonardo Murialdo, 1 I-00146 Roma, Italy
[5] Centre de Recherche sur la Synthèse et la Chimie des Mineraux, C.N.R.S., 1A rue de la Férollerie, F-45071 Orléans Cedex 2, France

Abstract—The reduction of hexavalent chromium species in aqueous solutions by interaction with Fe(II)-bearing solid surfaces was studied using a 0.96×10^{-3} M Cr(VI) solution and iron-rich clays with different Fe(II)/Fe(III) ratios, layer charge, and exchange properties, *i.e.*, chlorite, corrensite, and montmorillonite. Experimental studies demonstrated that Fe(II)-bearing phyllosilicates reduce aqueous Cr(VI) ions at acidic pH. Chlorite and corrensite, owing to the high Fe(II)/Fe(III) ratio, are electrochemically reactive, as rapid Cr(VI) reduction indicated. In contrast, montmorillonite showed minimum to nil reactivity towards Cr(VI). Furthermore, corrensite, which is high in both Fe(II)/Fe(III) ratio and exchange capacity, adsorbs the greatest amount of chromium.

X-ray absorption spectroscopy at Al, Mg, Fe, and Cr K-edges was used to investigate the adsorbed chromium species. The montmorillonite sample, unaffected by treatment with Cr(VI) solution, displays no change at any investigated edge. Edge shape and energy also do not change for the Mg and Al spectra in corrensite, and changes are minor in chlorite. By contrast, the Fe K-edge changes both in chlorite and corrensite, and indicates an increase of Fe(III) in treated samples at the expense of pre-existing Fe(II). Cr K-edge spectra show that chlorite and corrensite sorb Cr(III), which implies its reduction from Cr(VI) in the interacting solution.

Key Words—Absorption, Chromium, EXAFS, Phyllosilicates, Reduction, XANES.

INTRODUCTION

The mechanisms by which toxic metal contaminants may be removed from aqueous solution by interaction with minerals include precipitation, cation exchange, and adsorption. Furthermore, mobility and sorption of transition metals depend upon the valence state. However, few studies have addressed the heterogeneous oxidation-reduction reactions that involve electron transfer between metals in solution and in soil minerals (White and Peterson, 1996; Ilton *et al.,* 1997; Peterson *et al.,* 1997). In this work, we examine the role of some Fe-rich phyllosilicates for the removal of hexavalent chromium species from aqueous solutions. Chromium(VI) widely occurs as pollutant associated with the heavy-metal industry and base-metal mining (Nriagu, 1988); therefore, it may be present as a contaminant in many soils, sediments, and groundwater. Chromium can exist in several valence states, with trivalent Cr(III) and hexavalent Cr(VI) being most common. These two oxidation states show different chemical, biological, and environmental properties (Felter and Dourson, 1997). Cr(III) is naturally present in the environment and, over the pH range of most natural groundwaters, is thermodynamically more stable as a sorbed surface complex or in a solid phase (such as an oxyhydroxide precipitate) than as an aqueous complex (Anderson, 1994; Gan *et al.,* 1996). Cr(VI), which is a known carcinogen (Felter and Dourson, 1997), is the more mobile and, potentially, the more biologically active of the two common oxidation states. It is a strong oxidizing agent and is thermodynamically stable as an anionic solution species [$(CrO_4)^{2-}$ or $(Cr_2O_7)^{2-}$] over the same pH range where Cr(III) tends to precipitate. Therefore, reactions that reduce Cr(VI) to Cr(III) are important because they may result in the conversion of a toxic, mobile element into a less toxic, immobile form.

Fe(II) is a ubiquitous potential agent for Cr(VI) fixation in natural systems, and the homogeneous reduction of chromate by divalent iron in aqueous solution [$Fe(II)_{(aq)}$] is well documented (Sedlak and Chan, 1997; Eary and Rai, 1988; Fendorf and Li, 1996). Moreover, experiments have provided evidence for the heterogeneous reduction of Cr(VI) by Fe(II)-bearing oxides, oxyhydroxides, and biotite (Peterson *et al.,* 1997; Charlet and Manceau, 1992). Indeed, Fe(II) in silicates may be an important reducing agent of Cr(VI) in aqueous systems, and it may be a more powerful reductant than $Fe(II)_{(aq)}$ (Deng and Stone, 1996; Eary and Rai, 1991). Fe(II) is abundant in many suboxic and anoxic soils and sediments, and it can be produced

Table 1. Chemical composition (oxide wt. %), cation-exchange capacity (CEC, meq/100 g), and formulae for chlorite, corrensite, and montmorillonite. The formulae were calculated by balancing the positive charges against 28, 25, and 22 negative charges in chlorite, corrensite, and montmorillonite, respectively.

	Chlorite	Corrensite	Montmorillonite
Oxide			
SiO_2	42.62	35.41	46.57
Al_2O_3	6.97	11.50	14.49
TiO_2	0.47	0.44	2.92
Fe_2O_3	5.42	4.12	11.03
Cr_2O_3	0.53	0.02	0.03
FeO	4.75	3.31	0.76
MgO	27.60	29.09	4.66
MnO	0.13	0.10	0.14
CaO	0.34	1.87	3.72
Na_2O	0.12	0.19	0.07
K_2O	0.01	0.02	0.90
H_2O	11.10	13.95	14.70
Total	100.06	100.02	99.99
CEC	10	40	70
Chemical formula (apfu)			
Si^{4+}	3.98	3.06	3.46
Al^{3+}	0.02	0.94	0.54
$^{[IV]}$total	4.00	4.00	4.00
Al	0.75	0.23	0.73
Ti	0.03	0.03	0.16
Fe^{2+}	0.33	0.21	0.04
Fe^{3+}	0.38	0.27	0.62
Cr^{3+}	0.04	0.003	0.002
Mg	3.84	3.75	0.52
Mn	0.01	0.02	0.01
$^{[VI]}$total	5.38	4.513	2.082
Ca	0.03	0.17	0.30
Na	0.02	0.03	0.01
K	0.00	0.00	0.09
$^{[XII]}$total	0.05	0.20	0.40
OH	8.00	5.00	2.00
O	10.00	10.00	10.00

also by photochemical reactions occurring in sunlit natural waters (Waite and Morel, 1988; Voelker and Sedlak, 1995; Kieber and Helz, 1992) or as bacterial reduction of crystalline Fe(III) oxides (Zachara *et al.*, 1998; Kostka and Nealson, 1995).

Reduction of Cr(VI) by Fe(II) involves three one-electron-transfer steps, with the rate of the reaction increasing at acidic pH (Sedlak and Chan, 1997):

$$Fe(II) + Cr(VI) \rightarrow Fe(III) + Cr(V) \quad (1)$$

$$Fe(II) + Cr(V) \rightarrow Fe(III) + Cr(IV) \quad (2)$$

$$Fe(II) + Cr(IV) \rightarrow Fe(III) + Cr(III) \quad (3)$$

In addition to pH, the rate of Cr(VI) to Cr(III) reduction is affected by numerous factors, such as the local groundwater and mineral chemistry, the solid and solution compositions of the waste or effluent, and the chemical changes over time as the reduction reaction progresses. In fact, all the original chemical features of a system may be extensively modified by secondary reactions with the rock or soil environment (Peterson *et al.*, 1997).

Iron-rich clay minerals are both potential reducing and binding agents for chromium. They can promote Cr(VI) to Cr(III) reduction and bind chromium species by electrostatic interactions on the permanent-charged sites, by covalent binding with hydroxyl groups, and by cation exchange. Therefore, phyllosilicates with different iron content, exchange properties, layer charge, and stacking, such as chlorite, corrensite, and montmorillonite, may affect both the reductive transformation reactions of chromium species and their migration differently.

The aims of the present study are: 1) to investigate the Cr(VI) to Cr(III) reduction in the presence of Fe-rich phyllosilicate minerals, in the absence of oxygen, and at acidic pH (~2.4) conditions, such as those found in some natural systems (*e.g.*, in a sunlit stream that receives significant input from acid-mine drainage); 2) to evaluate the extent and the rate of reduction; 3) to determine the Cr species present and the mode of sorption or precipitation on minerals; and 4) to determine if Fe(II) in minerals can be oxidized to Fe(III) by reaction with Cr(VI)-bearing solutions.

To achieve these aims we reacted three Fe-rich minerals with solutions containing Cr(VI) and studied the products by a variety of methods, including X-ray absorption spectroscopy (XAS).

MATERIALS AND METHODS

Three iron-rich clays, an iron-rich montmorillonite, a chlorite, and a regularly interstratified chlorite-smectite (corrensite), were selected on the basis of dissimilar 1) Fe(II)/Fe(III) ratio, and 2) adsorption and exchange properties owing to differences in the chemistry of the 2:1 layer and in the interlayer. Differences in the interlayer are related to the presence of an octahedral interlayer sheet in chlorite, cations and water molecules in montmorillonite, and chlorite-like interlayers alternating with interlayers of cations and water molecules in corrensite.

The iron-rich montmorillonite was collected from weathered basaltic rocks from Campotamaso Valdagno, Berici Hills, Vicenza Province, Italy, and the chlorite and corrensite samples are from altered serpentinites near Borgotaro, Taro Valley, Parma Province, Italy. Chemical composition, cation-exchange capacity (CEC), and chemical formulae are given in Table 1. Chemistry was obtained by X-ray fluorescence (Philips, PW 1400) and Fe(II)/Fe(III) ratio by a semi-microvolumetric method (Meyrowitz, 1970). The water content was obtained by the weight loss of thermogravimetric analyses [simultaneous DTA-TGA Seiko SSC 5200 apparatus, heating rate 10°C min^{-1}, in air and in argon flow (50 mL min)] and was corrected assuming a complete Fe(II) oxidation during heating. We recognize, however, that such estimates could be affected

https://doi.org/10.1346/CCMN.2000.0480214 Published online by Cambridge University Press

by errors originating from the latter assumption. CEC was calculated following the method of Bergaya and Vayer (1997).

Chlorite and corrensite are commonly trioctahedral. However, the Borgotaro chlorite shows an incomplete brucite-like layer ($^{VI}\Sigma$ = 5.38) and a limited cation exchange, which suggests that alteration occurred after formation (Table 1). The octahedral positions of both chlorite and corrensite are occupied mainly by Mg, which is substituted by Fe(II) and Fe(III) [(Fe(II)/Fe(III) = 0.87 and 0.78 in chlorite and corrensite, respectively]. Minor Cr, Mn, and Ti substitutions are present also. The montmorillonite is dioctahedral, with Fe(III) substituting for Al in octahedral sites, and with low Fe(II) content [Fe(II)/Fe(III) = 0.06].

X-ray diffraction (XRD) analysis (Philips PW 900 diffractometer, CuKα radiation at room temperature and at 60% relative humidity) was performed on randomly oriented and oriented clay-aggregate mounts. Results indicate that there are no detectable crystalline impurity phases. However, to further purify the minerals, the samples were separated magnetically and treated with 1 M NaCl solution. With the latter procedure, the Na-exchanged clays may be easily separated from associated impurities (Amrhein and Suarez, 1991). Afterwards, to obtain interlayer features more similar to natural material, each sample was treated with 1 M $CaCl_2$ solution three times at 24-h intervals. Then the clays were dialyzed with distilled water until chloride free. Finally, the salt-free samples were dried and stored at room temperature.

Stock potassium-dichromate solutions (0.96×10^{-3} M) were prepared by dissolving $K_2Cr_2O_7$ analytical-grade reagents and then by filtering through 0.2-μm membrane filters prior to use. The pH of the solution was adjusted to 2.4 using H_2SO_4 (96%).

Experiments were performed using samples weighing 4.36 g in polyethylene reactors with 1000 mL of 0.96×10^{-3} M hexavalent-chromium solution. The amount of mineral to use in each experiment was determined by balancing the stoichiometry of the reaction $6Fe^{2+} + Cr_2O_7^{2-} + 14H^+ \rightarrow 6Fe^{3+} + 2Cr^{3+} + 7H_2O$ on the basis of chlorite. Chlorite has the highest Fe(II) content of our samples, and this stoichiometry was maintained constant for corrensite and montmorillonite also. All suspensions were purged with argon for ~30 min to reduce the partial pressure of CO_2, the reactors were closed, protected from light, and shaken continuously at room temperature (25 ± 1°C) for 1 wk, then at 70 ± 1°C for 1 d. Aliquots of the suspensions were collected at regular time intervals ranging from 5 min up to 4 d, using a polyethylene syringe through a Teflon valve, and pH was measured concurrently. The solid and the supernatant solution were immediately separated by centrifugation and analyzed for total Cr and Cr(VI). Na, Ca, Mg, and Si were determined for the final solutions to determine mineral dissolution.

For each supernatant, total Cr, Na, Ca, and Mg were determined by inductively coupled plasma spectroscopy (ICP, Varian Liberty 200) and Si was analyzed by UV-visible spectrophotometry (Varian DMS 70). To evaluate the Cr(VI)-Cr(III) reduction, the Cr(VI) content of the solution was determined by the 1,5 diphenylcarbazide-colorimetric method (APHA, 1989).

The filtrates were analyzed by powder X-ray diffraction, thermogravimetric analyses, and X-ray absorption near-edge structure (XANES) spectroscopy. All X-ray absorption experiments were performed at Stanford Synchrotron Radiation Laboratory (SSRL) with the electron-storage ring operating at 3 GeV and the electron current decaying from 100 to 60 mA. Fluorescence-yield K-edge spectra were taken for Fe at beam line SBO4-1, which is equipped with a double-crystal Si (111) monochromator. The beam line produces a resolution of ~1.5 eV. Spectra were recorded at steps of 0.35 eV for 1 s using a Lytle detector and soller slits, and with the sample compartment filled by He (Lytle *et al.*, 1984). For Cr, beam line SBO4-13 was used with a 13-element Ge detector. Resolution was ~1.0 eV. We recorded at 0.30 eV steps for 1 s per step. These beam lines extract synchrotron radiation (SR) by a wiggler to produce extremely high signal-to-noise ratios. Thin films of each sample were prepared on X-ray transparent Kapton tape, and two pieces of this tape were superposed and mounted on sample holders. Absorption data were collected at room temperature in air. Calibration for energy was made with a standard Fe metal foil for Fe and with Cr_2O_3 for Cr. The Al and Mg K-edge measurements were performed on beam line SBO3-3, which uses a bending magnet under high vacuum to extract SR from the ring. This beam line uses the JUMBO monochromator equipped with a double-crystal YB_{66} cut along the (400) plane (Wong *et al.*, 1999). Spectra acquisition ranged from 1540 to 1690 eV for Al and from 1280 to 1360 eV for Mg, with counting at 0.3–0.5 eV intervals for 2–4 s. Specimen preparation consisted of powdered samples (3 mg) mounted directly on flat Ag-coated slides after dispersion in acetone (5 mL). Akermanite ($Ca_2Mg_2Si_2O_7$) and Al metal foil were used as reference compounds to calibrate Mg and Al, respectively. The recorded spectra were energy-corrected as a function of the ring current, fitted with a Victoreen polynomial function to account for the base line, and normalized to 1 at high energy (50 eV above threshold, Bianconi, 1988) according to algorithms developed and commonly used for dichroism experiments (Chaboy *et al.*, 1998). These algorithms are able to detect changes in the peak signal in the order of 10^{-3}–10^{-4}.

Chromium(VI) compounds used for XAS modeling and pre-edge height calibration include Na_2CrO_4 and

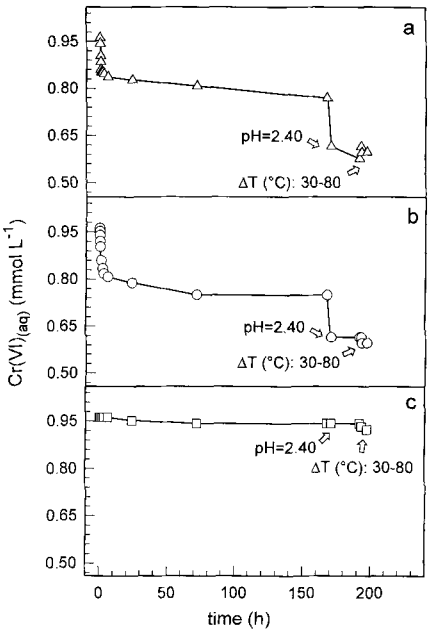

Figure 1. Plots of $[Cr(VI)_{(aq)}]$ (mmol L^{-1}) detected in solution *vs.* time (h) for: a) chlorite, b) corrensite, and c) montmorillonite. ΔT (°C): temperature range used in the treatment.

$SrCrO_4$ analytical reagents. The Cr(III) model compounds are synthetic Cr_2O_3 and uvarovite from Outukumpu, Finland.

RESULTS AND DISCUSSION

The amount of Cr(VI) detected in solution $[Cr(VI)_{(aq)}]$ as a function of time, for the three solution-mineral systems, is reported in Figure 1. For chlorite (Figure 1a) and corrensite (Figure 1b), an initial, rapid, and substantial decrease in $[Cr(VI)_{(aq)}]$ is followed by a gradual and nearly negligible decrease, whereas for montmorillonite the reaction is slow (Figure 1c). Experimental data are well fitted (≤168 h) by Equation (4) for chlorite and Equation (5) for corrensite:

$$[Cr(VI)_{(aq)}] = 0.1139 \times \exp(-4.5t) + 0.8480 - 4.6 \times 10^{-4}t \quad (4)$$

$$[Cr(VI)_{(aq)}] = [0.21/(t + 1)^{0.75}] + 0.75 \quad (5)$$

where t is time in hours and $[Cr(VI)_{(aq)}]$ is the chromium concentration in solution (mmol L^{-1}) (Figure 2). During the first 2 h, $[Cr(VI)_{(aq)}]$ reduction is more rapid in the chlorite system. Soon after, Cr(VI) reduction becomes linear with time [rate of the reaction 4.6×10^{-4} mmol L^{-1} h^{-1}; Equation (4)]. The corrensite system shows an initial reduction of Cr(VI), slower than for chlorite. With time, the rate of the reaction decreases further. The system reaches an asymptotic value after ~72 h. Within the first 30 min of reaction, the plots of $\ln[Cr(VI)_{(aq)}]$ *vs.* time become linear for chlorite ($y = -0.21432x - 5.234 \times 10^{-2}$; correlation coefficient, $r = -0.969$, Figure 3a) indicating that the reaction is first order (rate constant, $k_{obs} = 0.204$ h^{-1}) with respect to $[Cr(VI)_{(aq)}]$. The reaction order differs for the corrensite system. During the first hour, a linear trend is observed in Figure 3b ($y = -0.1581x - 4.04 \times 10^{-2}$; $r = -0.998$) where a plot of $\ln[Cr(VI)_{(aq)}]$ *vs.* ln time (order of the reaction = 7.32) is given. Deviations from first order indicate that either the reaction order with respect to $[Cr(VI)_{(aq)}]$ is >1.0, or other phenomena cause the reaction rate to diminish. The reaction products show the following: 1) Mg, Ca, Si, and Fe contents of the final solutions indicate that congruent dissolution occurs in corrensite, whereas, the high Mg

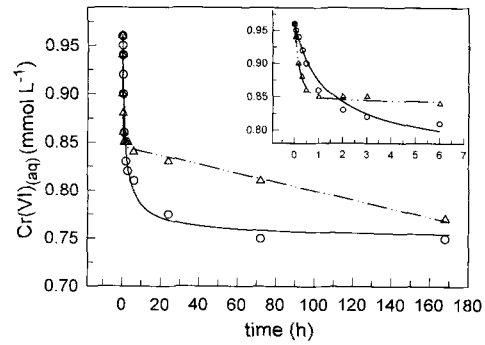

Figure 2. Plot of fitting curves for $[Cr(VI)_{(aq)}]$ (mmol L^{-1}) *vs.* time in chlorite (dash-point-point line and triangles) and corrensite (solid line and circles).

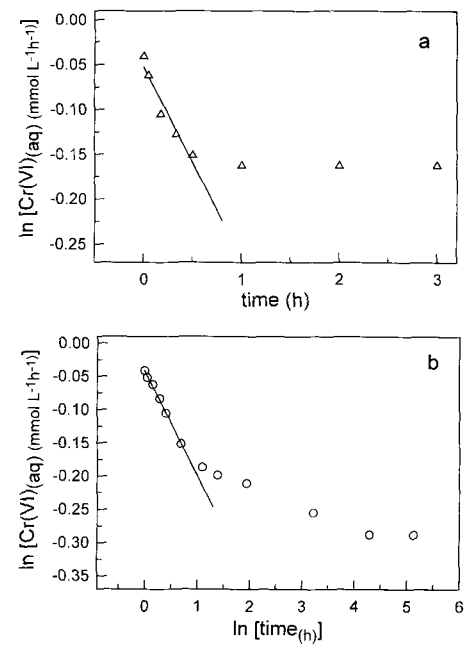

Figure 3. Plots of a) $\ln[Cr(VI)_{(aq)}]$ *vs.* time for chlorite and b) $\ln[Cr(VI)_{(aq)}]$ *vs.* ln time for corrensite. The calculations for kinetics used only the first five points for chlorite and the first six points for corrensite.

https://doi.org/10.1346/CCMN.2000.0480214 Published online by Cambridge University Press

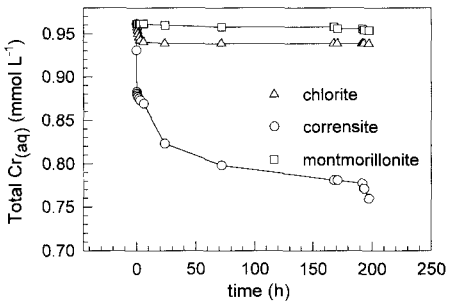

Figure 4. Plots of total Cr (mmol L^{-1}) in solution *vs.* time (h) for chlorite, corrensite, and montmorillonite.

content of the chlorite system suggests an incongruent dissolution mostly related to cations of octahedral coordination; 2) adsorption of Cr(III) decreases Cr(VI) reduction and/or adsorption, thus leading to a lower decrease in $[Cr(VI)_{(aq)}]$ as a function of time. Figure 4 shows that total chromium in solution (total $Cr_{(aq)}$) decreases slightly when in contact with montmorillonite and chlorite, whereas a large amount of total $Cr_{(aq)}$ is removed by corrensite.

Comparison of Figures 1 and 2 with Figure 4 suggests that: 1) the chlorite system, which has a low CEC of 10 meq/100 g and a high Fe(II) content (0.33 atoms per formula unit, apfu), shows a reaction mostly involving Cr(VI) reduction; 2) the montmorillonite system, which has low Fe(II) content (0.04 apfu) and a high CEC of 70 meq/100 g, shows a low Cr(VI) to Cr(III) reduction and has adsorption reactions that may suggest that hexavalent chromium species do not easily enter the interlayer; 3) the corrensite system, which has both a notable Fe(II) content at 0.21 apfu and a significant CEC of 40 meq/100 g, shows Cr(VI) to Cr(III) reduction and that all Cr species present are adsorbed simultaneously.

After 2 d of treatment, the pH of each system slightly increases and after 140 h was 3.5 for chlorite, 3.3 for corrensite, and 3.0 for the montmorillonite system. Therefore, because Cr(VI) reduction is favored at very low pH, each system was acidified using H_2SO_4 after 150 h of reaction. This procedure adjusted the pH to the initial pH value (2.4) and allowed the mineral substrates to further reduce Cr(VI). Indeed, after acidification, the corrensite and chlorite systems were still able to reduce Cr(VI) (Figure 1a and 1b), although changes in Cr(VI) content were not observed for montmorillonite (Figure 1c). Afterwards, in all systems, Cr(VI) reduction attains steady-state levels within 24 h and also the increase of temperature up to 70°C does not reveal significant Cr(VI) reduction. Maximum Fe(II) oxidation occurs at room temperature (FeO in wt. % remaining in chlorite = 3.17, corrensite = 1.70, montmorillonite = 0.60), whereas only a limited amount of Fe(II) is oxidized at 70°C (FeO in wt. % remaining in chlorite = 3.05; corrensite = 1.65; montmorillonite = 0.55).

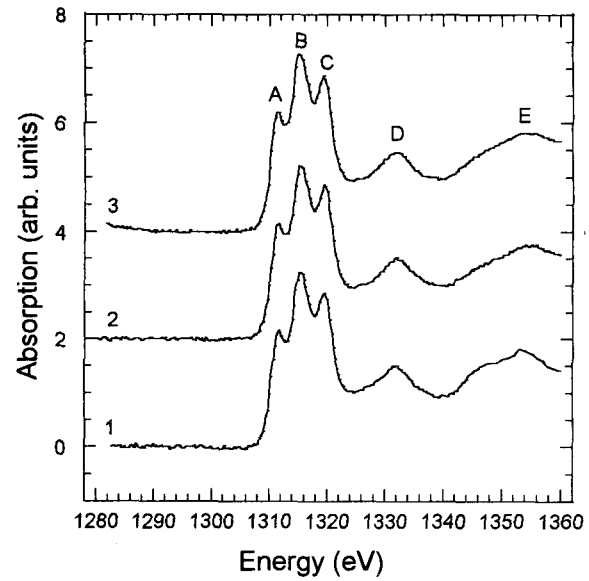

Figure 5. XANES spectra at the Mg K-edge for corrensite. Labels of tracings: 1) untreated sample; 2) mineral portion treated at room temperature with 0.96 mmol L^{-1} Cr(VI) solution at ≤170 h; 3) the same mineral portion acidified to pH = 2.4 and heated to 70°C (see Figure 1).

XAS is useful to determine oxidation, coordination, and the local environment of Cr in the phyllosilicates before and after interaction with the Cr(VI)-bearing solution. The Mg K-edge spectra of chlorite, corrensite, and montmorillonite are similar and do not change with the treatment (see corrensite Mg K-edge spectra, curves 2 and 3, Figure 5). Chlorite and corrensite spectra display three well-resolved peaks in the edge region at 1310 (label A), 1314 (label B), and 1318 (label C) eV, and broader resonances at higher energy near 1330 and 1350 eV (labels D and E). In both spectra, pre-peak features are absent, which is consistent with regular octahedral coordination. In particular, the phyllosilicate spectra strongly resemble those of talc (Wong *et al.*, 1994; *cf.* Figure 5), where Mg occupies regular octahedral sites. In montmorillonite, the low Mg content (Table 1) produces a very low signal-to-noise ratio. However, observed peak energies do not differ substantially from those of chlorite and corrensite.

Aluminum K-edge spectra were recorded also before and after the reactions (Figure 6). Chlorite and corrensite show spectra with three peaks in the edge region: two well-resolved peaks at 1566 and 1572 eV (labels A and B, respectively) and a weak shoulder near 1575 eV (label B′). A very broad band centered near 1588 eV (label C) occurs also. In montmorillonite two peaks (labels A and B) at 1568 eV and 1574 eV, respectively, and the broad band (label C) centered at

https://doi.org/10.1346/CCMN.2000.0480214 Published online by Cambridge University Press

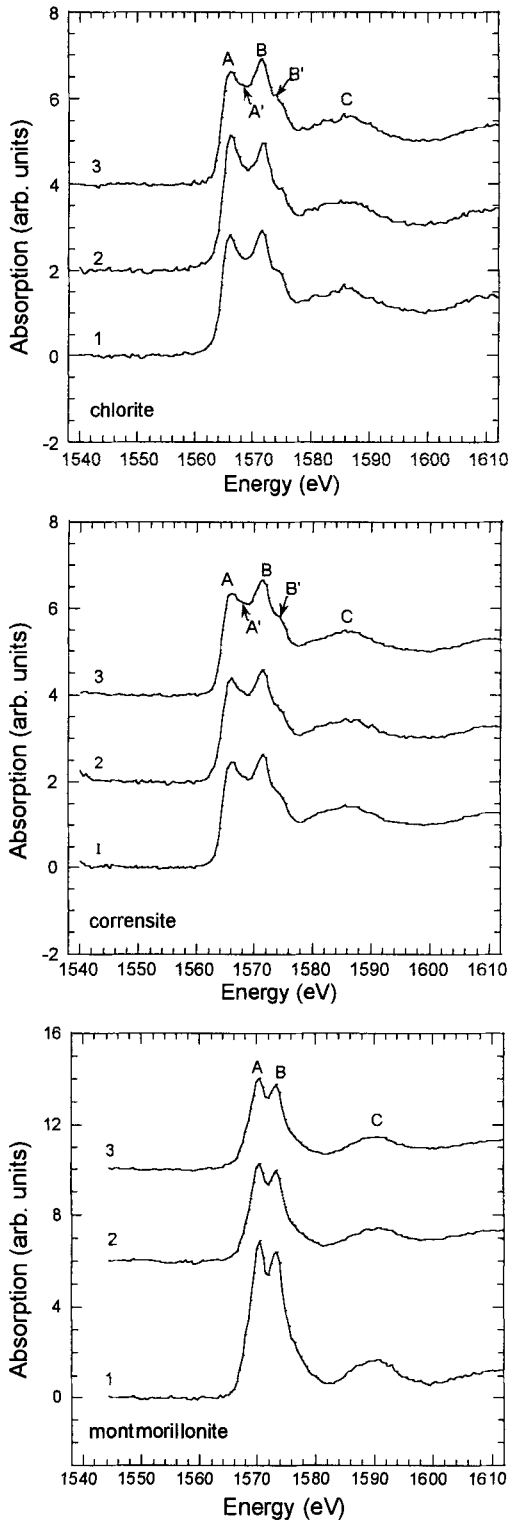

Figure 6. XANES spectra at the Al K-edge for chlorite, corrensite, and montmorillonite. Labels of tracings 1, 2, and 3 as in Figure 5.

1590 eV are present, whereas the shoulder (label B′) is poorly defined or sometime nonexistent. In corrensite and in chlorite treated at 70°C, a very broad peak (label A′) occurs at 1568 eV (equal energy as the A peak of montmorillonite). In chlorite, the spectral shape changes after treatment; the A peak (1566 eV) decreases in intensity with respect to the B peak (1572 eV), although peak energies remain the same. The B′ and C bands are unchanged. These results suggest that no significant change in the structure of the 2:1 phyllosilicate layer occurs, but there is a rearrangement of the Al in the octahedral sheet as a result of treatment with Cr solutions.

The shape of the chlorite spectrum after the treatment is similar to that of corrensite. This feature is consistent with chlorite having incongruent dissolution which causes an increase of smectite-type interlayers. Furthermore, a small XRD peak at ~29 Å and an endothermic reaction at 170°C, are suggestive of a smectite-like interlayer.

The Fe K-edge spectra for all the phyllosilicates (Figure 7) was possible because each contained sufficient iron. Generally (*e.g.*, Calas *et al.*, 1980; Bonnin *et al.*, 1985), although the edge shapes may vary, the spectrum of Fe(III) consists of three features: a pre-edge at 7113–7113.7 eV, a broad maximum or shoulder between 7122–7123.3 eV, and an edge crest at 7128–7132.3 eV. In contrast, the spectrum of Fe(II) usually consists of four well-defined features: the 1*s*-3*d* absorption at 7111.1–7112.1 eV, two strong edge features at 7118.0–7120.7 eV and 7123–7125 eV, and the edge crest at 7128–7129.4 eV. Furthermore, as with all transition elements, tetrahedrally coordinated Fe(III) displays a stronger pre-edge than octahedral iron (Dräger *et al.*, 1988).

The weak pre-edges in the spectra of the phyllosilicates suggest that Fe is present only in octahedral coordination, but they are sufficiently broad that the determination of energy, and thus oxidation state, is not possible. Positions and intensities of the main edge features are similar for chlorite and corrensite and consist of a relatively sharp absorption edge with a maximum at 7129–7130 eV (label A) and a small shoulder at ~7127 eV (label A′). In addition, there is a feature near 7143–7145 eV (label B), plus two broad features at higher energy (labels C and D). Montmorillonite spectrum consists of three features: a peak at 7133 eV (label A), a shoulder at 7148 eV (label B), and a very broad band (label C) with maximum between 7180–7190 eV. The observed spectra confirm that Fe is present in all three phyllosilicates as both Fe(II) and Fe(III) ions. However, Fe(II) is predominant in chlorite and corrensite, and Fe(III) dominates in montmorillonite, in agreement with chemical data and results from similar smectites (Bonnin *et al.*, 1985; Paris *et al.*, 1991). Figure 7 also shows that the absorption features of montmorillonite, which has the least Fe(II) and

https://doi.org/10.1346/CCMN.2000.0480214 Published online by Cambridge University Press

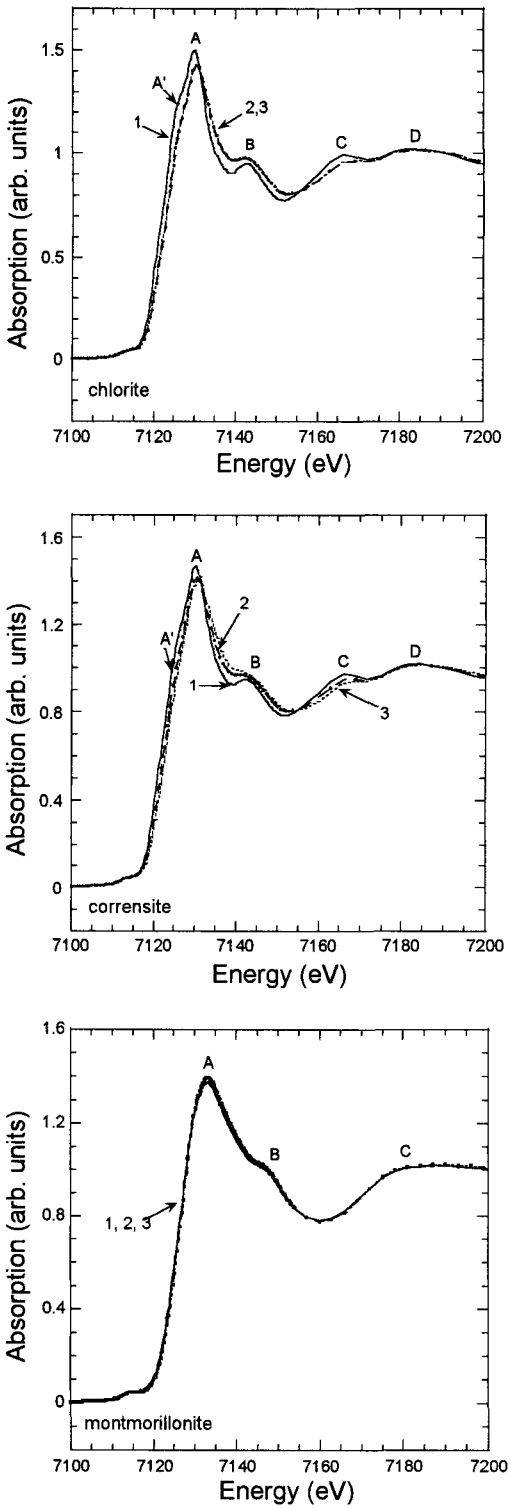

Figure 7. XANES spectra at the Fe K-edge for chlorite, corrensite, and montmorillonite. Solid line refers to untreated sample (label 1), point-line to sample treated at room temperature with 0.96 mmol L^{-1} Cr(VI) solution for ≤170 h (label 2), dash-line to the same sample acidified to pH = 2.4 and heated to 70°C (label 3). See Figure 1 also.

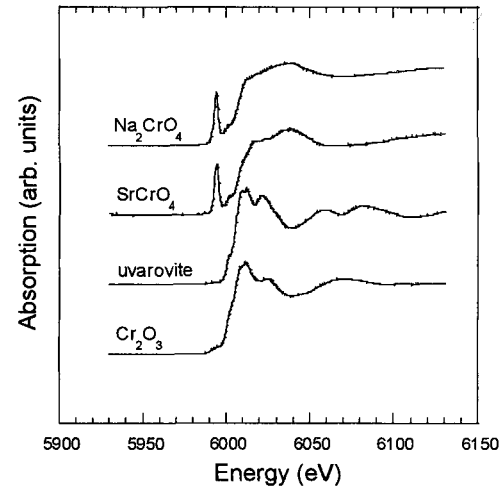

Figure 8. XANES spectra at the Cr K-edge for model compounds.

therefore the smallest Cr(VI) reduction capacity, are nearly the same before and after treatment. In contrast, the absorption features of chlorite and corrensite display changes with treatment suggesting that structural Fe(II) is affected by the Cr(VI) to Cr(III) reduction proces. In chlorite, the edge top shifts to lower energy (−2 eV) with increasing treatment, whereas features A′ and B become less resolved. If the general relations given above are correct, these changes imply that a portion of the initial Fe(II) is oxidized. Disorder of Fe in octahedral sites increases as indicated also by the smoothing of spectral features for the treated sample when compared to the untreated sample. However, the patterns are nearly similar before and after heat treatment (with only small changes for corrensite), thereby suggesting that Fe is reacting in corrensite by an interaction with the Cr(VI) solution, whereas later heating does not affect significantly the montmorillonite and chlorite systems. Nevertheless, the observed changes suggest that Fe(II) is important in Cr reduction at the chlorite and corrensite mineral substrate, and that it contributes to the reduction of aqueous Cr(VI) to Cr(III).

The K-edge high-resolution spectra for chromium model compounds are given in Figure 8. Figure 9 shows the experimental chromium spectra for the three phyllosilicates. Changes in Cr oxidation state are recognized by shifts in the absorption edge energy. The energy of the valence orbitals and, therefore, the energy position of the edge and pre-edge features are correlated with the valence state of Cr in the sample. Each absorption feature is shifted to higher energies with increasing Cr oxidation state (Bajt *et al.*, 1993). For example, the energy of the edge inflection point of the model compounds $SrCrO_4$ and Na_2CrO_4, both containing Cr(VI), shift ~5 eV toward higher energies

https://doi.org/10.1346/CCMN.2000.0480214 Published online by Cambridge University Press

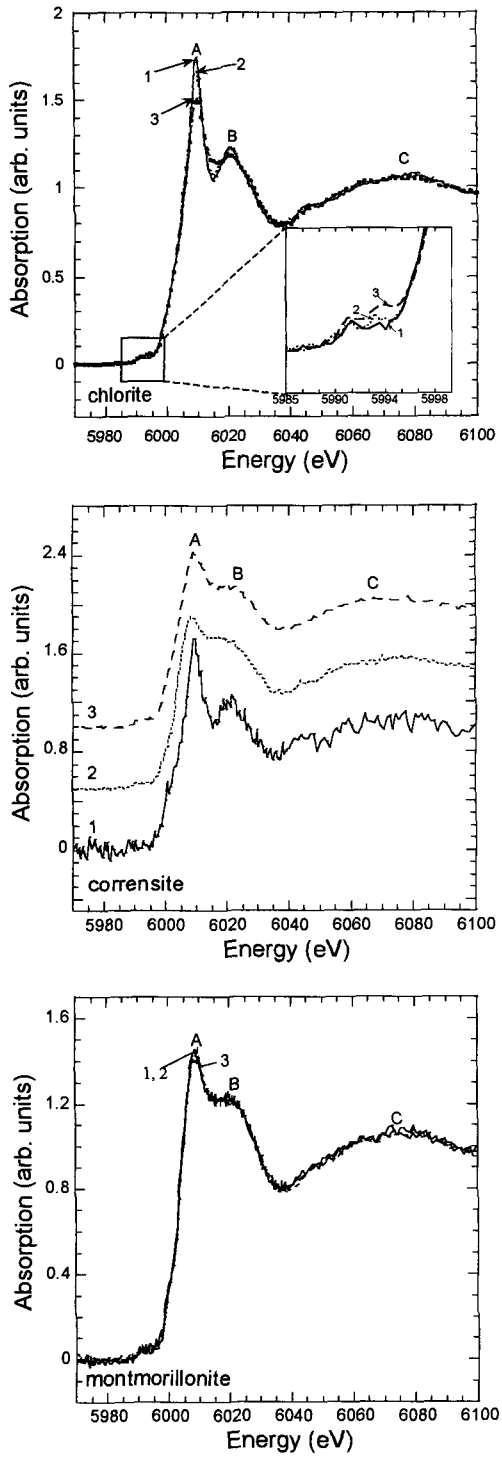

Figure 9. XANES spectra at the Cr K-edge for chlorite, corrensite, and montmorillonite. Labels of tracings as in Figure 7.

with respect to the position of the edge for Cr_2O_3 and uvarovite, both containing Cr(III) (Figure 8). Symmetry changes at the site occupied by Cr affect the entire edge, with marked changes on the edge shape (Bianconi, 1988). For example, Cr in tetrahedral coordination exhibits a single intense pre-edge peak and a small shoulder at ~10 eV above the pre-edge (Bianconi, 1988; Bianconi *et al.,* 1992; Bajt *et al.,* 1993). These typical pre-edge features are found in the reference $SrCrO_4$ and Na_2CrO_4 compounds (Figure 8), where Cr was shown by structure determination to be four-coordinated (Arcon *et al.,* 1998; Munoz-Paez *et al.,* 1995). The octahedral site is recognized by the lack of a pre-edge peak (Cr_2O_3 and uvarovite spectra, Figure 8) and by two small resonances in the pre-edge region (Bajt *et al.,* 1993; Arcon *et al.,* 1998).

Figure 9 is consistent with the chemical data (Table 1) that Cr is present in small amounts in chlorite. However, the Cr content is much lower in corrensite and montmorillonite; note the differences in background and signal-to-noise ratios for untreated phyllosilicates. The Cr spectra show an absorption edge inflection at 6005 eV, a broad main edge at 6010 eV (label A), a higher energy, broad peak (label B) at 6020 eV (in chlorite), or a shoulder (in corrensite and montmorillonite), and a very broad band centered at ~6075 eV (label C). Comparison of Figures 8 and 9 suggests that chromium is present in all untreated samples as Cr(III) in octahedral coordination. In fact, all spectra strongly resemble the Cr_2O_3 model spectrum (Figure 8). After treatment, the edge-tops (label A) decrease in intensity for chlorite and corrensite, whereas the 6020-eV feature becomes weaker, although always well resolved in chlorite. In corrensite the 6020-eV feature also weakens, but the resolution increases. In contrast, in montmorillonite this feature remains a broad shoulder. There are variations also in the pre-edge features. In untreated chlorite, the pre-edge features are at 5990 and 5994 eV, but in the chlorite after heating, the Cr K-edge spectrum shows a new feature on the rising limb of the main absorption peak. Figure 9 also indicates that Cr mostly affects the spectrum of the corrensite sample with increasing treatment. In this case, the background decreases and the signal quality increases markedly from tracing 1 to 3. The observed data are consistent with Cr(VI) being reduced to Cr(III) before sorption on phyllosilicates. Unfortunately, these XANES spectra are not of sufficient quality to determine if (Mg, Fe)Cr_2O_4 precipitates on the surface, if Cr substitutes in octahedral or interlayer sites, or if both may occur. The broadening of the B peaks suggests that Cr substitutional disorder occurs in the layer structure. However, a small amount of Cr(VI) may remain in the treated samples.

SUMMARY AND CONCLUSIONS

After reaction with Cr(VI) in aqueous solutions, Fe-rich phyllosilicates reduce the total amount of Cr(VI)

https://doi.org/10.1346/CCMN.2000.0480214 Published online by Cambridge University Press

in the following order: chlorite ≅ corrensite ≫ montmorillonite. The rate of reduction depends on Fe(II) content. Reduction is more rapid initially and slows considerably with treatment.

After reduction, Cr is sorbed or precipitated as Cr(III) primarily in octahedral coordination. The mechanisms by which chromium is reduced-sorbed by the phyllosilicates remain unknown. The mineral structures are maintained during the experiments, as indicated by XANES analysis. The montmorillonite system with low Fe(II) content is unaffected by treatment, whereas chlorite and corrensite show changes in the Al, Fe, and Cr spectra. A portion of the mineral sample dissolves during treatment; therefore, in addition to reactions involving external surfaces, we cannot exclude the possibility of the occurrence of charge-balancing reactions within the mineral, presumably involving the octahedral and interlayer sites.

Because Cr(III)-bearing clay minerals can both reduce Cr(VI) to Cr(III) and adsorb Cr(III) as a function of layer charge, the materials may be useful in reducing Cr toxicity in environments contaminated by Cr(VI).

ACKNOWLEDGMENTS

XAS experiments were performed at the Stanford Synchrotron Radiation Laboratory (SSRL), which is supported by the Department of Energy, Office of Basic Energy Sciences, and is operated by Stanford University. The Italian MURST (project "Layer silicates: Crystal chemical, structural and petrological aspects") and CNR supported our research program both abroad and at home. Specials thank to S. Fendorf and to S. Guggenheim who made useful suggestions for improving the paper.

REFERENCES

Amrhein, C. and Suarez, D.L. (1991) Sodium-calcium exchange with anions exclusion and weathering corrections. *Soil Science Society of America Journal,* **55,** 698–706.

Anderson, R.A. (1994) Nutritional and toxicological aspects of chromium intake: An overview. In *Risk Assessment of Essential Elements,* W. Mertz, C.O. Abernathy, and S.S. Olin, eds., ILSI Press, Washington, D.C., 187–196.

APHA, AWWA, WPC (1989) *Standard Methods for Examination of Water and Wastewaters, 17th edition.* American Public Health Association, Washington D.C., 201–204.

Arcon, I., Mirtic, B., and Kodre, A. (1998) Determination of valence states of chromium in calcium chromate by using X-ray adsorption near edge structure (XANES) spectroscopy. *Journal of American Ceramic Society,* **81,** 222–224.

Bajt, S., Clark, S.B., Sutton, S.R., Rivers, M.L., and Smith, J.V. (1993) Synchrotron X-ray microprobe determination of chromate content using X-ray absorption near edge structure. *Analytical Chemistry,* **65,** 1800–1804.

Bergaya, F. and Vayer, M. (1997) CEC of clays: Measurement by adsorption of a copper ethylenediamine complex. *Applied Clay Science,* **12,** 275–280.

Bianconi, A. (1988) XANES Spectroscopy. In *X-ray Absorption: Principles, Applications, Techniques of EXAFS, SEXAFS and XANES,* D.C. Konigsberger and R. Prins, eds., Wiley, New York, 573–662.

Bianconi, A., Garcia, J., Benfatto, M., Marcelli, A., Natoli, C.R., and Ruiz-Lopez, M.F. (1992) Multielectron excitation in the K-edge X-ray absorption near edge spectra of V, Cr, and Mn $3d^0$ compounds with tetrahedral coordination. *Physical Review B: Condensed Matter,* **13,** 6885–6892.

Bonnin, D., Calas, G., Suquet, H., and Pezerat, H. (1985) Site occupancy of Fe^{3+} in Garfield nontronite: A spectroscopic study. *Physics and Chemistry of Minerals,* **12,** 55–64.

Calas, G., Levitz, P., Petian, J., Bondot, P., and Loupias, G. (1980) Etude de l'ordre local autour du fer des verres silicates naturales et synthetiques a l'aide de la spectrometrie d'absorption X. *Review Physical Application,* **15,** 1161–1167.

Chaboy, J., Garcia, M.L., Bartolome, F., Marcelli, A., Cibin, G., Maruyama, H., Pizzini, S., Rogalev, A., Goedkoop, J.B., and Goulon, J. (1998) X-ray magnetic-circular-dichroism probe of a noncollinear magnetic arrangement below the spin reorientation transition in $Nd_2Fe_{14}B$. *Physical Review B: Condensed Matter,* **57,** 8424–8429.

Charlet, L. and Manceau, A. (1992) X-ray absorption spectroscopic study of the sorption of Cr(III) at the oxide-water interface. *Journal of Colloid Interface Science,* **148,** 443–458.

Deng, B.L. and Stone, A.T. (1996) Surface catalyzed chromium (VI) reduction—the TiO_2-Cr(VI) mandelic acid system. *Environmental Science and Technology,* **30,** 463–472.

Dräger, G., Frahm, R., Materlik, G., and Brümmer, O. (1988) On the multiple character of the X-ray transition in the pre-edge structure of Fe K absorption spectra. An experimental study. *Physica Status Solidi (B),* **149,** 287–294.

Eary, L.E. and Rai, D. (1988) Chromate removal from aqueous wastes by reduction with ferrous ions. *Environmental Science Technology,* **22,** 972–977.

Eary, L.E. and Rai, D. (1991) Chromate reduction by subsurface soils under acidic conditions. *Journal of Sciences and Technology,* **22,** 972–977.

Felter, S.P. and Dourson, M.L. (1997) Hexavalent chromium-contaminated soils: Option for risk assessment and risk management. *Regulatory Toxicology and Pharmacology,* **25,** 43–59.

Fendorf, S.E. and Li, G. (1996) Kinetics of chromate reduction by ferrous ions. *Environmental Science and Technology,* **30,** 1614–1617.

Gan, H., Bailey, G.W., and Yu, S.Y. (1996) Morphology of lead(II) and chromium(III) reaction products on phyllosilicate surfaces as determined by atomic force microscopy. *Clays and Clay Minerals,* **44,** 734–743.

Ilton, E.S., Veblen, D.R., Moses, C.O., and Raeburn, S.P. (1997) The catalitic effect of sodium and lithium ions on coupled sorption-reduction of chromate at the biotite edge-fluid interface. *Geochimica et Cosmochimica Acta,* **61,** 3543–3563.

Kieber, R.J. and Helz, G.R. (1992) Indirect photoreduction of chromium (VI). *Environmental Science and Technology,* **26,** 307–312.

Kostka, J.E. and Nealson, K.H. (1995) Dissolution and reduction of magnetite by bacteria. *Environmental Science and Technology,* **29,** 2535–2540.

Lytle, F.W., Greegor, R.B., Sandtrom, D.R., Marques, E.C., Wong, J., Spiro, C.L., Huffman, G.P., and Huggins, F.E. (1984) Measurement of soft X-ray absorption spectra with a fluorescence ion chamber detector. *Nuclear Instrument and Methods in Physical Research,* **A 226,** 542–548.

Meyrowitz, R. (1970) A semimicroprocedure for the determination of ferrous iron in non-refractory silicate minerals. *American Mineralogist,* **48,** 298–310.

Munoz-Paez, A., Pappalardo, R.R., and Sanchez Marcos, E. (1995) Determination of the second hydration shell of Cr^{3+} and Zn^{2+} in aqueous solution by extended X-ray absorption fine structure. *Journal of the American Chemical Society,* **117,** 11710–11720.

Nriagu, J.O. (1988) Production and use of chromium. In *Chromium in the Natural and Human Environments,* J.O. Nriagu and E. Nieboer, eds., Wiley, New York, 81–104.

Paris, E., Mottana, A., and Mattias, P. (1991) Iron environment in a montmorillonite from Gola del Furlo (Marche, Italy). A synchrotron radiation XANES and a Mössbauer study. *Mineralogy and Petrology,* **45,** 105–117.

Peterson, M.L., Brown, G.E., Parks, G.A., and Stein, C.L. (1997) Differential redox and sorption of Cr(III/VI) on natural silicate and oxide minerals: EXAFS and XANES results. *Geochimica et Cosmochimica Acta,* **61,** 3399–3412.

Sedlak, D.L. and Chan, P.G. (1997) Reduction of hexavalent chromium by ferrous iron. *Geochimica et Cosmochimica Acta,* **61,** 2185–2192.

Voelker, B.M. and Sedlak, D.L. (1995) Iron photoreduction by photoproduced superoxide in seawater. *Marine Chemistry,* **50,** 93–102.

Waite, T.D. and Morel, F.M.M. (1988) Photoreductive dissolution of colloidal iron oxides in natural waters. *Environmental Science Technology,* **18,** 860–868.

White, A.F. and Peterson, M.L. (1996) Reduction of aqueous transition metal species in the surfaces of Fe(II)-containing oxides. *Geochimica et Cosmochimica Acta,* **60,** 3799–3814.

Wong, J., George, G.N., Pickering, I.J., Rek, Z.U., Rowen, M., Tanaka, T., Via, G.H., DeVries, B., Vaughan, D.E.W., and Brown, G.E., Jr. (1994) New opportunity in XAFS investigation in the 1–2 keV region. *Solid State Communications,* **92,** 559–562.

Wong, J., Tanaka, T., Rowen, M., Schafers, F., Muller, R.B., and Rez, Z.U. (1999) YB_{66}—A new soft X-ray monochromator for synchrotron radiation. II. Characterization. *Journal of Synchrotron Radiation,* **6,** 1086–1095.

Zachara, J.M., Fredrickson, J.K., Li, S.M., Kennedy, D.W., Smith, S., and Gassman, P. (1998) Bacterial reduction of crystalline Fe^{3+} oxide in single phase suspensions and subsurfaces materials. *American Mineralogist,* **83,** 1426–1443.

E-mail of corresponding author: brigatti@unimo.it

(Received 3 May 1999; accepted 6 December 1999; Ms. 339; A.E. William F. Bleam)